

Flat, C^{α,β}-Didehydroalanine Foldamers with Ferrocene Pendants: Assessing the Role of α -Peptide Dipolar Moments

Saverio Santi,^{*[a]} Annalisa Bisello,^[a] Roberta Cardena,^[a] Silvia Tomelleri,^[a] Renato Schiesari,^[a] Barbara Biondi,^[b] Marco Crisma,^[b] and Fernando Formaggio^{*[a,b]}

[a] Prof. S. Santi, Dr. A. Bisello, Dr. R. Cardena, Dr. S. Tomelleri, Dr. R. Schiesari, Prof. F. Formaggio
Department of Chemical Sciences
University of Padova
via Marzolo 1, 35131 Padova, Italy
E-mail: saverio.santi@unipd.it; fernando.formaggio@unipd.it

[b] Dr. B. Biondi, Dr. M. Crisma, Prof. F. Formaggio
Institute of Biomolecular Chemistry, Padova Unit, CNR
via Marzolo 1, 35131 Padova, Italy

Supporting information for this article is given via a link at the end of the document.

Abstract: The foldamer field is continuously expanding as it allows to produce molecules endowed with 3D-structures and functions never observed in Nature. We synthesized flat foldamers based on the natural, but non-coded, C^{α,β}-didehydroalanine α -amino acid, and covalently linked to them two ferrocene (Fc) moieties, as redox probes. These conjugates retain the flat and extended conformation of the 2.0₅-helix, both in solution and in the crystal state (X-ray diffraction). Cyclic voltammetry measurements agree with the adoption of the 2.0₅-helix, characterized by a negligible dipole moment. Thus, this type of elongated, α -peptide stretches are insulators rather than charge conductors, the latter being constituted by peptide α -helices. Also, our homo-tetrapeptide has a N-to-C length of about 18.2 Å, almost double that (9.7 Å) of an α -helical α -tetrapeptide.

Introduction

Proteins are *natural* foldamers^[1] that for millions of years have been supporting life. Surprisingly, despite the large variety of functions exerted, proteins are based on only twenty monomers, fished out among the hundreds of naturally available α -amino acids. Thus, a huge, unexplored ground is offered to chemists.^[2] Indeed, the advancements of synthetic chemistry has allowed the introduction of a considerable number of *artificial* foldamers, endowed with structures and functions never observed before.^[1b,3] However, efforts are continuously made also to mimic protein functions, but using β -, γ - and δ -amino acids,^[3e,4] as well as other non-coded α -amino acids.^[5] These residues are investigated for a variety of reasons: they impart enzymatic resistance to the peptides where they are inserted;^[5j] they are contained in bioactive natural products;^[5k] they increase peptide structural rigidity;^[4] they are useful tools to build new 3D-structures;^[4b,5b] they can be exploited in bio-organic and supramolecular chemistry.^[5c-e,5l]

In this contribution we exploit the C^{α,β}-didehydroalanine (Δ Ala) residue, a natural α -amino acid^[6] not belonging to the protein pool. We took advantage of its peculiar conformational preference^[7] to deepen our knowledge on the charge/electron transfer mediated

by proteins. To this aim, we synthesized a series of Δ Ala homopeptides bearing two ferrocene (Fc) groups at their ends (Figure 1). Δ Ala is known to preferentially adopt the *fully-extended* conformation. This 3D-structure, not common in proteins,^[8] is also known as 2.0₅-helix because it is characterized by 2 residues per turn and stabilized by H-bonds encompassing 5-membered pseudo-cycles (Figure 1).^[7-9] In this peculiar type of helix the rotation per residue along the helix axis is exactly 180°.

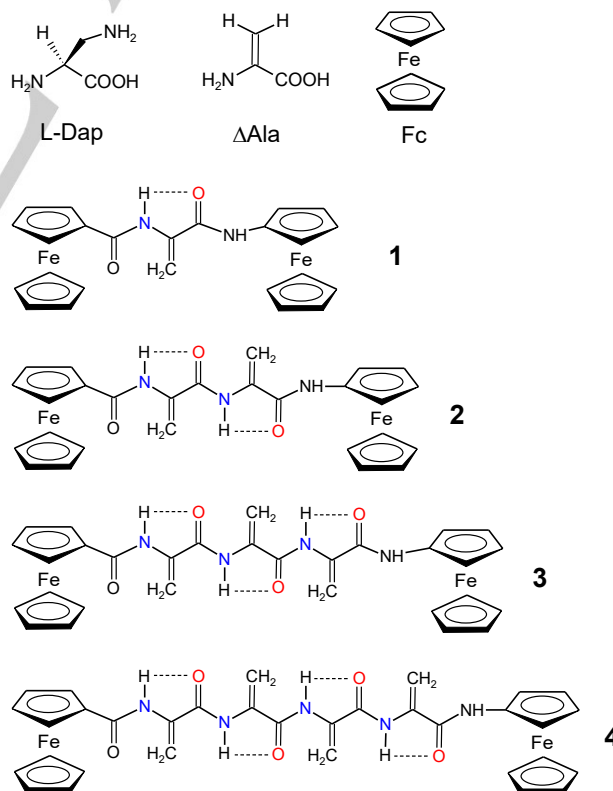


Figure 1. Chemical structures of Dap, Δ Ala, Fc and of the Fc/peptide conjugates synthesized in this work. Intra-residue H-bonds are indicated by dashed lines.

As a result, Δ Ala stretches arrange as flat foldamers. The 2.0_5 -helix displays two other interesting features: (i) the N-to-C termini distance is the longest an α -peptide can span, almost double than that of an α -helix (Figure 2); (ii) at variance from α - or 3_{10} -helices, in which all C=O groups are nearly parallel to the helix axis and point toward the C-terminus, thus generating a macro-dipole moment the magnitude of which depends on the helix length, the C=O are arranged perpendicularly to the long axis of the 2.0_5 -helix and with alternate orientations (Figure 2); thus, a macro-dipole moment cannot be generated along the helix axis, and perpendicularly to it the individual C=O dipoles sum up to zero if their number is even. We exploited this second feature to corroborate the significance of the dipole moment in promoting charge transfer in helical peptides and proteins.^[10] The covalently bound Fc moieties function as redox probes.

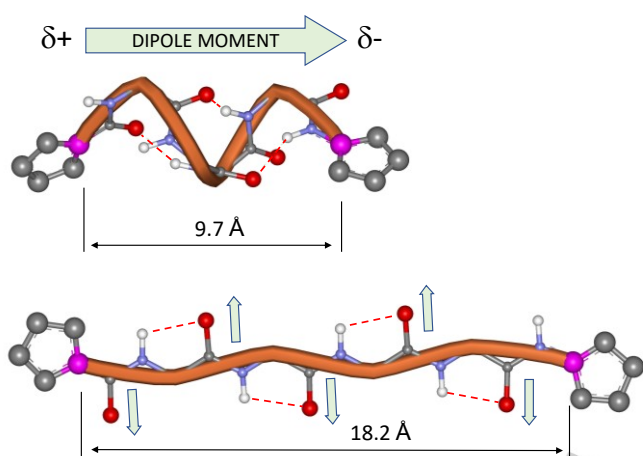


Figure 2. Molecular models of Fc-CO-(Δ Ala)₄-NH-Fc folded as an α -helix (top) and a 2.0_5 -helix (fully-extended conformation, bottom). For clarity, the side chains are omitted and the two Fc moieties are represented by cyclopentenes. The three *intra*-molecular (top) and the four *intra*-residue (bottom) H-bonds are represented by dashed lines.

Covalent pathways and intramolecular hydrogen bonds facilitate electron or charge migration in folded polypeptides, through *superexchange* or *hopping* mechanisms.^[11] In this connection, peptide helices are crucial for long-range electron transfer.^[12] Bioorganometallic compounds, particularly bioconjugates of ferrocene with amino acids and peptides, have found extensive application in studying charge transfer processes in proteins but also molecular electronics, conductive nanostructures, peptide-based nanomaterials or materials for biomedical use.^[13] The redox-active components allow to get insights on the 3D-structures of the foldamers and on the elements responsible for donor...acceptor interactions. Fc derivatives are useful tools for the labeling of biomolecules. Indeed, they have an excellent stability in different environments (e.g., in solution and in air) and they easily undergo chemical modifications without losing their well-defined electrochemical features.^[14] Moreover, Fc can be exploited to inject a positive charge and to map its delocalization in the peptide chains.^[15]

A number of literature reports deal with Fc-containing peptides, with contribution from our^[15] and other laboratories.^[11f,13c,14,16] In particular, self-assembling Fc-peptides were proposed as ideal candidates to understand charge/electron motion along polypeptide chains.^[17] It was observed that in α -helices ultra-long-

range electron hopping can occur (up to 100 Å). Our present contribution deals for the first time with the behavior of the fully-extended (2.0_5 -helix) peptide conformation in charge/electron transfer processes.

Results and Discussion

Peptide synthesis

For the synthesis of Fc-CO-(Δ Ala)_n-NH-Fc ($n = 1-4$) we relied on a previously exploited strategy,^[7] that foresees the synthesis of the precursor peptide series Fc-CO-(L-Dap)_n-NH-Fc ($n = 1-4$; Dap, 2,3-diaminopropionic acid) followed by the Hoffman elimination. Minor modifications were applied in the coupling reactions of Fc and Dap. Briefly, Z-L-Dap(Boc)-OH (Z, benzyloxycarbonyl; Boc, *t*-butyloxycarbonyl) was coupled to ferrocenyl amine by means of EDC [N-ethyl-N'-(3-dimethylamino-propyl)carbodiimide] and HOBT (1-hydroxybenzotriazole) to obtain Z-L-Dap(Boc)-NH-Fc. After removal of the Z protecting group by catalytic hydrogenolysis, a second Z-L-Dap(Boc)-OH derivative was introduced, again mediated by the EDC/HOBT activating mixture. The same two steps (hydrogenolysis and EDC/HOBT coupling) were repeated on the obtained dipeptide, Z-[L-Dap(Boc)]₂-NH-Fc, to prepare the tripeptide and the tetrapeptide and to introduce the N-terminal Fc-COOH moiety in all four peptides. Yields were generally good and only in the case of the introduction of Fc-COOH a purification step *via* medium pressure chromatography was required. Finally, the four Fc-CO-[L-Dap(Boc)]_n-NH-Fc ($n = 1-4$) conjugates were individually treated with trifluoroacetic acid, to remove the Boc protecting groups from the side chains, and used for the subsequent reaction without further purification. Treatment of the side-chain, free amines with CH₃I and KHCO₃ in a methanol/dimethylformamide mixture allowed us to obtain Fc-CO-(Δ Ala)_n-NH-Fc ($n = 1-4$) in acceptable yields (40 to 60%).

Conformational analysis in solution

We performed a conformational analysis in CDCl₃ solution by means of NMR and IR absorption spectroscopies. The most informative bands in the IR spectra (Figure 3) clearly indicate that peptides **1-4** adopt the fully-extended conformation, stabilized by intra-residue H-bonds. Indeed, in the amide A region (Figure 3 top) we observe for all peptides a band at about 3450 cm⁻¹, ascribable to the stretching of the solvated, non H-bonded, C-terminal N-H (*i.e.*, the amide NH-Fc). All remaining amide NHs are involved in a H-bond, centered at about 3385 cm⁻¹. The position of this absorption calls for a weak H-bond, such as that of the intra-residue, C₅ conformation.^[7] In addition, at variance from α (or 3_{10})-helical peptides, where by lengthening the peptide this band moves to lower wavenumbers in view of a cooperative effect of the increasing number of H-bonds, in the fully-extended conformation this stabilizing effect is not operative because the H-bonds are intra-residue. In the tri- and tetrapeptide some aggregation occurs, as highlighted by the wide bands at about 3300 cm⁻¹. Aggregation in peptides is commonly due to intermolecular N-H...O=C interactions. However, in this case we cannot rule out the possibility of π -stacking of some ferrocene moieties. Indeed, an extensive π -stacking is observed in the packing mode of the crystal structure of the dipeptide (see Supporting Information).

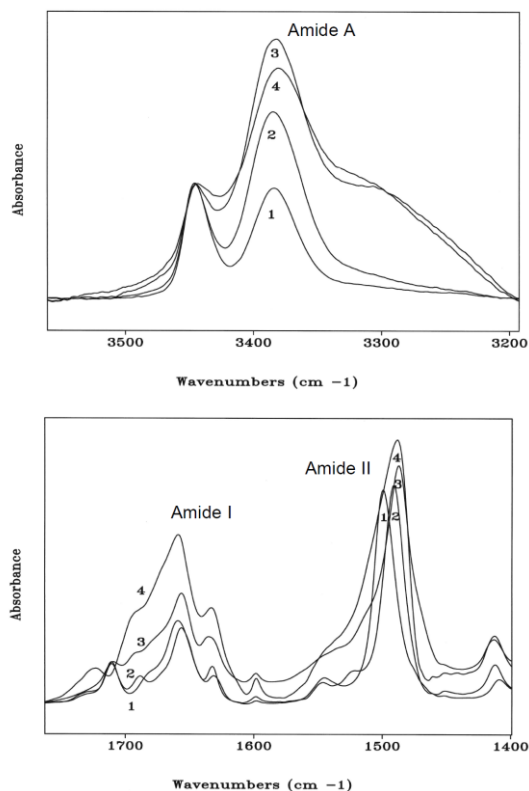


Figure 3. FT-IR absorption spectra of Fc-CO-(Δ Ala) $_n$ -NH-Fc ($n = 1, 4$) in the amide A (top) and amide I and II (bottom) regions. Peptide concentration: 1 mM in CDCl₃.

An inspection to the amide I (~ 1650 cm⁻¹) and amide II (~ 1500 cm⁻¹) regions of the IR spectra (Figure 3 bottom) allows us to corroborate the hypothesis that peptides **1–4** adopt the fully-extended conformation. In general, α (or 3_{10})-helical peptides display the amide I band at about 1665 cm⁻¹ and a less intense amide II band at about 1515 cm⁻¹.^[18] On the other hand, in peptides adopting the fully-extended conformation (i) the intensity of the amide II band (~ 1500 cm⁻¹) is higher than that of the amide I (~ 1660 cm⁻¹) and (ii) the amide II band falls below 1500 cm⁻¹.^[9f–j] These features are clearly observed in the IR spectra of peptides **1–4**. Interestingly, the amide II absorption frequencies move to lower wavenumbers going from peptide **1** to peptide **4** (1500, 1491, 1487, and 1485 cm⁻¹, respectively). We tentatively attribute this shift to the (alkene)C-H \cdots O=C H-bonds (see the crystal-state section), as the stretching of the amide C-N, that contributes as much as 40% to the amide II band, may be favored when the amide C=O is involved in two H-bonds (with the intra-residue N-H and with the alkene C-H of the following residue).

The conclusions of this IR absorption analysis are confirmed by the NMR analyses (Figures 4 and 5) performed in the same solvent. To a 1 mM solution of the peptides in CDCl₃ we added increasing amounts of dimethylsulfoxide (DMSO), a strong H-bond acceptor. As a result, the amide protons not involved in H-bonds moved downfield in the NMR spectra, whereas those H-bonded were little affected. In peptides **1–4** only the C-terminal amide NH (-NH-Fc) is sensitive to the perturbing solvent. This behavior is indicative of the adoption of the 2.0₅-helix, where all Δ Ala amide NHs are involved in *intra*-residue H-bonds. As representative examples, we report the experiments performed on compounds **3** and **4** (Figure 4).

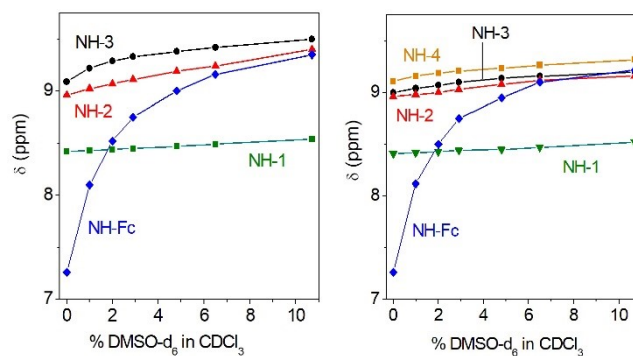


Figure 4. Chemical shift variations of the amide NHs upon addition of increasing percentages of DMSO- d_6 to CDCl₃ solutions of Fc-CO-(Δ Ala)₃-NH-Fc (left) and Fc-CO-(Δ Ala)₄-NH-Fc (right). Peptide concentration: 1 mM.

To correctly assign the resonances we exploited homo- and hetero-correlated 2D-NMR experiments. This work, in turn, allowed us to detect for peptides **1–4** patterns of connectivities typical of the fully-extended conformation.^[9f] In particular, all cross peaks between an H of the Δ Ala β -CH₂ group and the proton N-H of the following residue are present. A region of the NOESY spectrum of Fc-CO-(Δ Ala)₃-NH-Fc is reported in Figure 5. Together with the β CH₂($i-1$)/NH(i) cross peaks, an interaction between the α C-H of the N-terminal Fc moiety (Fc1) and the N-H of Δ Ala1 is also evident.

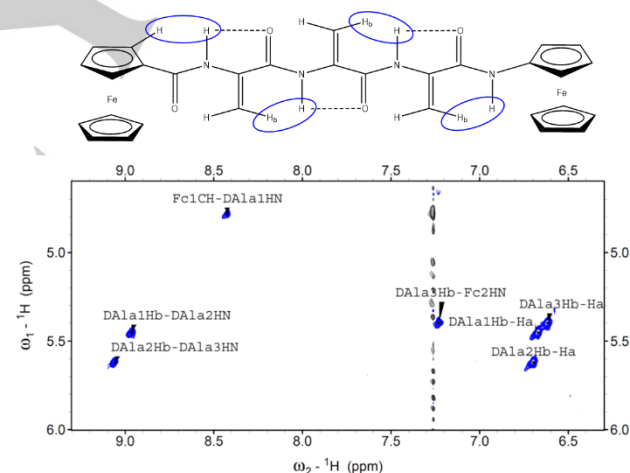


Figure 5. β CH \rightarrow NH region of the NOESY spectrum of Fc-CO-[Δ Ala]₃-NH-Fc in CDCl₃ solution, T = 25 °C.

Crystal-state conformation

The molecular structures of Fc-CO- Δ Ala-NH-Fc and Fc-CO-(Δ Ala)₂-NH-Fc, as determined by single crystal X-ray diffraction analysis, are illustrated in Figure 6 and 7, respectively. In the structure of Fc-CO- Δ Ala-NH-Fc, two crystallographically independent molecules (A and B in Figure 6) compose the asymmetric unit.

In both structures, the two cyclopentadienyl rings of each Fc unit are parallel to each other (the angle between normals to their average planes is within 3.7°), and they are found in a nearly eclipsed disposition, the largest value among the average interring H-C \cdots C-H twist angles, 12.3°, being found for the C-terminal

Fc unit of Fc-CO-(Δ Ala)₂-NH-Fc. Such geometrical features are quite common for monosubstituted Fc derivatives.^[19]

Bond distances and bond angles of the Δ Ala residues are in general agreement with previously reported values for this C $^{\alpha}$,C $^{\beta}$ unsaturated residue.^[7,8] In particular: (i) The average N-C $^{\alpha}$ bond distance, 1.399 Å, is significantly shorter than that typical for peptides based on coded amino acids (1.46 Å),^[20] whereas the effects of the *sp*² hybridization of the C $^{\alpha}$ atom and the possible π -electron delocalization seem to be less pronounced on the average length of the Δ Ala C $^{\alpha}$ -C bond, 1.511 Å, with respect to the corresponding bond in regular peptides (1.53 Å).^[20] (ii) The values of the N-C $^{\alpha}$ -C bond angle of Δ Ala residues, ranging from 107.5° to 109.3°, are significantly compressed with respect to the typical bond angles for an *sp*² hybridized, trisubstituted carbon atom (120°).

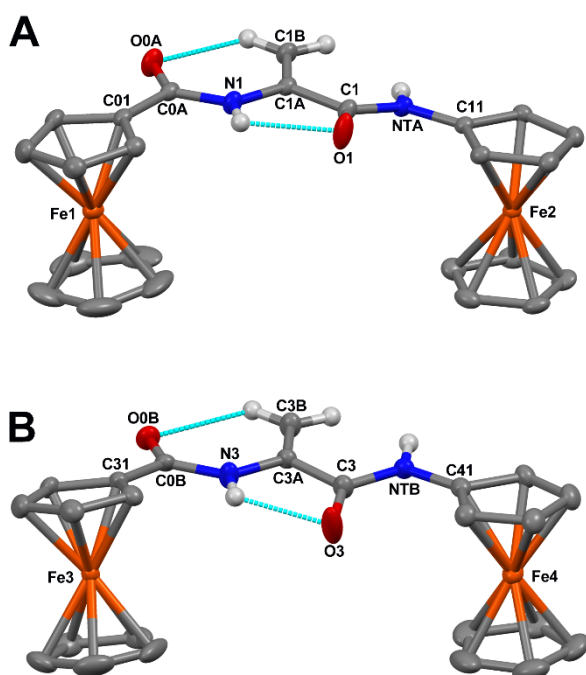


Figure 6. X-Ray diffraction structure of Fc-CO- Δ Ala-NH-Fc with atom numbering. The two crystallographically independent molecules are indicated with **A** and **B**, respectively. Anisotropic displacement ellipsoids for the non-H atoms are displayed at the 30% probability level. H-atoms of the ferrocene units are omitted for clarity. The intramolecular N-H...O=C and C-H...O=C H-bonds are indicated by dashed lines.

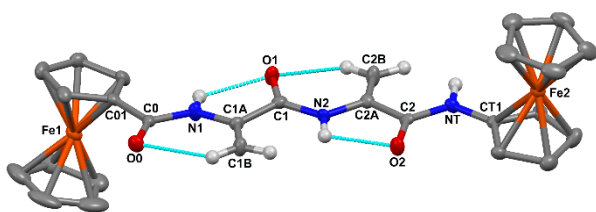


Figure 7. X-Ray diffraction structure of Fc-CO-(Δ Ala)₂-NH-Fc with atom numbering. Anisotropic displacement ellipsoids for the non-H atoms are displayed at the 30% probability level. H-atoms of the ferrocene units are omitted for clarity. The intramolecular N-H...O=C and C-H...O=C H-bonds are indicated by dashed lines.

Both structures are characterized by a fully-extended conformation of the peptide backbone.^[8] All of the ϕ , ψ , and ω torsion angles, including the ω_0 and ω_T torsion angles at the level of the N-terminal and C-terminal amide bonds, respectively, show values close to 180° (Supporting Information, Tables S1 and S3). The largest deviation from exact *trans*-planarity, observed for the ψ value of molecule B in Fc-CO- Δ Ala-NH-Fc, does not exceed 10.8°. The fully-extended conformation is stabilized by intramolecular H-bonds between the N-H and C=O groups of the same Δ Ala residue, thus closing a five-atom *pseudocycle* (C₅ structure), one in each independent molecule of Fc-CO- Δ Ala-NH-Fc (Figure 6) and two in the dipeptide (Figure 7). The H...O distances are in the range 2.08 - 2.15 Å, and the values of the N-H...O angles are between 110.3° and 112.4° (Supporting Information, Tables S2 and S4). Although, in general, N-H...O=C interactions featuring N-H...O angles less than 120° are not usually considered to be H-bonds, there is spectroscopic and computational evidence for the true H-bond nature of the C₅ structure.^[8,21] In addition to the intra-residue N-H...O=C H-bonds, intramolecular C-H...O=C H-bonds are also observed (Figures 6 and 7 and Supporting Information, Tables S2 and S4), each of them involving a hydrogen atom of the Δ Ala β -CH₂ group as the donor and the preceding carbonyl oxygen atom as the acceptor. Such a fully extended conformation and the related intramolecular H-bonding network is typical for Δ Ala homo-peptides.^[7]

In each structure, the proximal (*i.e.* directly connected to the peptide backbone) cyclopentadienyl rings of the N- and C-terminal ferrocene moieties are essentially coplanar to the peptide backbone. Specifically, the angles between the normal to the backbone average plane and the normals to the proximal cyclopentadienyl rings of respectively the N- and C-terminal Fc units are: 13.2° and 7.1° in molecule A of Fc-CO- Δ Ala-NH-Fc; 13.5° and 2.8° in molecule B; 14.1° and 7.7° in the dipeptide.

The most striking difference between the two structures is the disposition of the two distal cyclopentadienyl rings with respect to the peptide backbone. They are placed on the same side in each independent molecule of Fc-CO- Δ Ala-NH-Fc (Figure 6), whereas in the dipeptide they point to opposite direction (Figure 7). This latter arrangement maximizes the distance between the Fe atoms of the N- and C-terminal Fc units. Indeed, the intramolecular Fe1...Fe2 separation, 13.749 Å, observed in the structure of Fc-CO-(Δ Ala)₂-NH-Fc is the largest possible for this type of ferrocene *bis*-derivatized dipeptide based on α -amino acids, as it results from the combination of the fully-extended conformation adopted by the peptide backbone with the antiverse disposition of the Fc units. Conversely, in the structure of Fc-CO- Δ Ala-NH-Fc the intramolecular Fe...Fe separations are 8.749 Å in molecule A and 8.645 Å in molecule B. It is possible that the *syn* disposition adopted by the terminal Fc units in both independent molecules may be related to packing requirements (see Supporting Information for details).

Cyclic voltammetry analysis

Ferrocene is an interesting redox probe as it is very stable in water and in the open air in both neutral and oxidized states, soluble in common organic solvents and endowed with a low oxidation potential. In this work, we exploited Fc to confirm the role of the peptide dipole moment in electrochemical processes. Indeed, some of us had already shown that the dipole moment of a 3₁₀-helical peptide strongly affects the redox potential of Fc moieties covalently bound to its N- and/or C-termini.^[15] In particular, the

change in the oxidation potential depends on the peptide terminus to which the Fc moiety is appended. As reported above, in an α (or 3_{10})-helix the amide C=O are roughly aligned along the helix axis, thus generating a positive pole at the N-terminus and a negative one at the C-terminus. Consequently, Fc is oxidized more easily when linked at the C-terminus. In addition, this effect becomes larger by lengthening the peptide, because of the additive contribution of increasing C=O dipoles with a potential variation of -66 mV along the series. The opposite is true when Fc is bound to the N-terminus ($+28$ mV).

Conversely, in a fully-extended peptide the C=O are arranged perpendicularly to the long axis of the 2.0_5 -helix and with alternate orientations. Therefore, we could predict that fully-extended peptides would not generate a macrodipole and not (or slightly) affect Fc oxidation. However, to the best of our knowledge no experimental evidence was so far produced. Our work aims at filling this gap and adding a new member to the foldamer ensemble.

The planar peptides **1–4** were studied by means of cyclic voltammetry measurements (Figure 8).

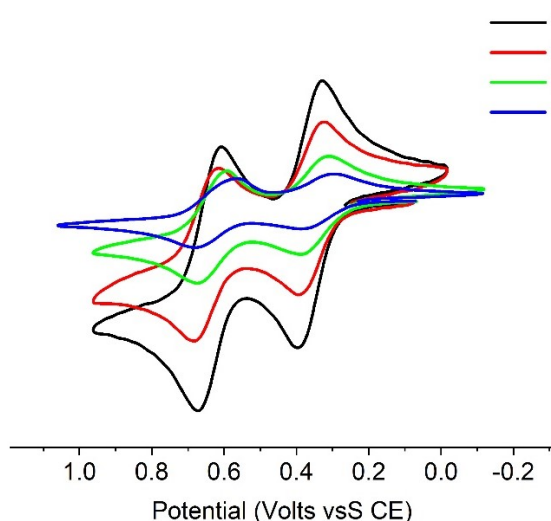


Figure 8. Cyclic voltammetry of the Fc-CO-(Δ Ala) $_n$ -NH-Fc ($n = 1-4$) series in CH_2Cl_2 containing 0.1 M $n\text{Bu}_4\text{NPF}_6$ as the supporting electrolyte [Au disk electrode ($d = 0.5$ mm); scan rate 0.2 Vs^{-1} ; T 20 $^\circ\text{C}$]. The current i is normalized according to the equation: $i \cdot v^{-1} \cdot c^{-1}$, with concentration c in the range $2.3-2.7$ mM.

Cyclic voltammograms, recorded under argon in 0.1 M CH_2Cl_2 / $n\text{Bu}_4\text{NPF}_6$, showed single oxidation waves of the Fc units, monoelectronic, chemically reversible, electrochemically reversible (**1** and **2**, $E_p - E_{p/2} = 60-70$ mV) and quasi-reversible (**3** and **4**, $E_p - E_{p/2} = 80-100$ mV) in the scan rate v between 0.1 and 5 Vs^{-1} , on a electrode gold disc working with diameter $d = 0.125$ mm ($0.5-5$ Vs^{-1}) and 0.5 mm ($0.1-0.5$ Vs^{-1}). It appears that the heterogeneous electron transfer rate decreases by increasing the length of the peptide chain.

The intensity of peak current (i_{max}) decreases along each peptide series, an effect due to the difference in the diffusion coefficients (D) as the number of residues varies. Indeed, in a cyclic voltammetry experiment $i_{\text{max}} \propto D^{1/2}$ and D depends on the molecular size, according to the Stokes-Einstein equation ($D \propto 1/r$). Lower values of D are expected for longer peptides, as a consequence of the fluid-dynamic effect. In general, large

molecules have a decreased mobility towards an electrode as compared to small molecules. The two Fc moieties in peptides **1–4** have different oxidation potentials as one Fc is functionalized with an electron-withdrawing group (C=O), the other with an electron-donating group (NH) (Figure 8). However, for both Fc the redox potentials are little sensitive to the length of the peptides showing a small variation of their $E_{1/2}$ (Figure 9). Indeed, the potential variation is -20 mV along the series when Fc is linked at the C-terminus, and -10 mV when Fc is bound to the N-terminus, within an experimental error $\delta E_{1/2} = \pm 10$ mV. These shifts are significantly smaller than those previously reported for 3_{10} -helical peptides, characterized by active dipole moments. Moreover, they have the same sign. Thus, they cannot be ascribed to the direction of an effective dipole moment of the peptides. In fact, in 3_{10} -helical peptides we previously observed a significant and continuous variation of $E_{1/2}$ as the peptide length was increased, positive and negative depending on the orientation of the dipole moment with respect to Fc.^[15]

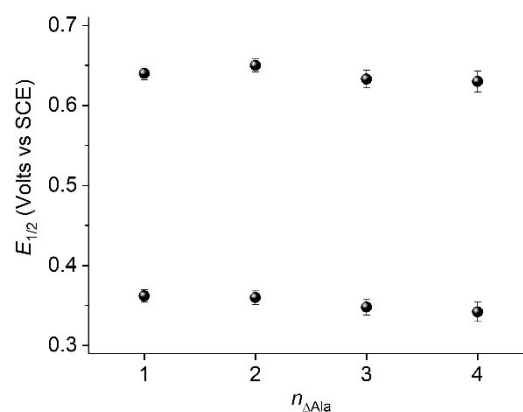


Figure 9. Plot of the oxidation potential $E_{1/2} [= E_p - (E_p - E_{p/2})/2]$, where E_p is the oxidation peak potential, $E_{p/2}$ the half-peak potential] reported in Figure 8 for the two Fc unities of peptides Fc-CO-(Δ Ala) $_n$ -NH-Fc ($n = 1-4$).

Therefore, this cyclic voltammetry study proves for the first time that peptides adopting the fully-extended conformation (2.0_5 -helix) have no dipole moment. As a corollary, the large influence exerted by helical peptides on the redox properties of covalently-bound Fc moieties are undoubtedly due the dipole moment of the peptide helix.

Conclusion

The foldamer field is constantly expanding due to the possibility to explore 3D-structures and functions not yet invented by Nature. In this work we added a piece of information to the field of foldamers based on α -peptides. By exploiting the natural, but non-coded, Δ Ala α -amino acid we synthesized its homopeptides up to the tetramer level and covalently linked to them two ferrocene (Fc) moieties. We demonstrated that these peptides adopt the fully-extended (2.0_5 -helix) conformation both in solution and in the crystal state. Interestingly, this flat structure remains stable even though two bulky Fc groups are appended to its ends. The Fc redox functionalities allowed us to indirectly support the

conclusion that the 2.0₅-helix does not possess a dipole moment. Thus, α -peptide stretches can be used as charge conductors, as Nature does with α -helices in some proteins, or as insulators, when elongated into a 2.0₅-helix. It would be fascinating to be able to reversibly guide a peptide from one to the other 3D-structure, as this capability would allow us to switch on and off a charge (or electron) transfer at the molecular level. In addition, it is worth mentioning that such a transition is also accompanied by a dramatic change of the peptide length (Figure 2): a peptide folded into an α -helix can almost double its length when stretched to a 2.0₅-helix.

Experimental Section

Synthesis. Experimental synthetic procedures for the synthesis of the fc/peptide conjugates and their characterization data are reported in the Supporting Information.

FT-IR analysis. The solution FT-IR absorption spectra were recorded at 293 K using a FT-IR Nicolet Nexus 670 spectrophotometer, nitrogen flushed, equipped with a sample-shuttle device, at 2 cm⁻¹ nominal resolution, averaging 25 scans. Solvent (baseline) spectra were recorded under the same conditions. Spectrograde CHCl₃-d (99.8%, d) was purchased from Sigma Aldrich. For spectral elaboration, the software SpectraCalc provided by Galactic (Salem, MA) was employed. Cells with path lengths of 1.0 and 10 mm (with CaF₂ windows) were used.

Nuclear Magnetic Resonance. ¹H and ¹³C NMR spectra were obtained on a Bruker Avance III HD spectrometer operating at 400.13 and 100.61 MHz, respectively (T = 298 K). The peptide concentration in solution was 1 mM in spectrograde CHCl₃-d₁ (99.8 % d, containing 0.5 %wt. of silver foils as stabilizers and 0.03 % (v/v) tetramethylsilane - Sigma Aldrich). Processing and evaluation of the experimental data were carried out using the TOPSPIN software packages. All homonuclear spectra were acquired by collecting 400 experiments, each consisting of 32 scans and 2K data points. The spin systems of the amino acid residues were identified using standard chemical shift correlation and 2D (NOESY, TOCSY and COSY) experiments. The 2D ¹H-¹³C correlation spectra HMQC and HMBC were recorded with 160 t₁ increments of 40-160 scans and 2K points each, using a spectral width of 180 ppm centred at 85 ppm in F₁.

X-Ray diffraction. Crystals of Fc-CO- Δ Ala-NH-Fc and Fc-CO-(Δ Ala)₂-NH-Fc were grown by slow evaporation from ethyl acetate / *n*-hexane and CHCl₃ / *n*-hexane solvent mixtures, respectively. X-Ray diffraction data were collected at room temperature with a Gemini E four-circle kappa diffractometer (Agilent Technologies) equipped with a 92 mm EOS CCD detector, using graphite monochromated Mo K α radiation (λ = 0.71073 Å). Data collection and reduction were performed with the CrysAlisPro software system (version 1.171.40.60a, Rigaku Corporation). A semi-empirical absorption correction based on the multi-scan technique using spherical harmonics, implemented in the SCALE3 ABSPACK scaling algorithm, was applied. Both structures were solved by *ab initio* procedures of the SIR 2014 program.^[22] Refinement was carried out by full-matrix least-squares on F², using all data, by application of the SHELXL-2014 program,^[23] with anisotropic displacement parameters for all of the non-H atoms. All cyclopentadienyl rings were constrained to the idealized geometry, and rigid-bond restraints were applied to the anisotropic displacement parameters of their carbon atoms. H-Atoms were calculated at idealized positions and refined using a riding model. Relevant crystal data and structure refinement parameters are listed below. CCDC 2034489 (Fc-CO- Δ Ala-NH-Fc) and 2034490 [Fc-CO-(Δ Ala)₂-NH-Fc] contain the supplementary crystallographic data for this paper. These data are provided free of charge by the joint Cambridge Crystallographic Data Centre and Fachinformationszentrum Karlsruhe Access Structures service www.ccdc.cam.ac.uk/structures.

Fc-CO- Δ Ala-NH-Fc. C₂₄H₂₂Fe₂N₂O₂. M = 482.13. Crystal dimensions 0.60 × 0.60 × 0.40 mm³. Monoclinic, space group P2₁/c. Unit cell dimensions: a = 14.0751(7) Å, b = 25.0570(12) Å, c = 12.7585(8) Å, β = 108.943(6)°. V = 4256.0(4) Å³. Z = 8. ρ_{calcd} 1.505 Mg/m³. λ = 0.71073 Å. μ = 1.386 mm⁻¹, min/max transmission 0.59436/1.0000. 47321 collected reflections, θ_{max} = 26.97°, 10216 independent reflections (R_{int} = 0.0485). Data / restraints / parameters 10216 / 252 / 469. Final R indices: R₁ = 0.0486 [*I* > 2 σ (*I*)], wR₂ = 0.1284 (all data). Goodness-of-fit on F² = 1.077. Residual electron density 0.698 / -0.653 e.Å⁻³.

Fc-CO-(Δ Ala)₂-NH-Fc. C₂₇H₂₅Fe₂N₃O₃. M = 551.20. Crystal dimensions 0.20 × 0.10 × 0.05 mm³. Orthorhombic, space group Pca2₁. Unit cell dimensions: a = 14.2249(8) Å, b = 6.4608(4) Å, c = 25.5990(13) Å. V = 2352.7(2) Å³. Z = 4. ρ_{calcd} 1.556 Mg/m³. λ = 0.71073 Å. μ = 1.269 mm⁻¹, min/max transmission 0.90058/1.0000. 17518 collected reflections, θ_{max} = 29.31°, 4270 independent reflections (R_{int} = 0.0675). Data / restraints / parameters 4270 / 121 / 280. Final R indices: R₁ = 0.0512 [*I* > 2 σ (*I*)], wR₂ = 0.1068 (all data). Goodness-of-fit on F² = 0.934. Residual electron density 0.526 / -0.375 e.Å⁻³.

Cyclic voltammetry. The measurements were performed in an air-tight three-electrode cell connected to a vacuum/argon line. The reference electrode was a SCE (Tacussel ECS C10) separated from the solution by a bridge compartment filled with the same solvent/supporting electrolyte solution used in the cell. The counter electrode was a platinum spiral with around 1 cm² apparent surface area. The working electrode was a disk obtained from cross section of a gold wire with 0.5 and 0.125 mm diameter sealed in glass. Between successive scans the working electrode was polished on alumina according to standard procedures and sonicated before use. An EG&G PAR-175 signal generator was used. The currents and potentials were recorded on a Lecroy 9310L oscilloscope. The potentiostat was home-built with a positive feedback loop for compensation of the ohmic drop.^[24]

Acknowledgements

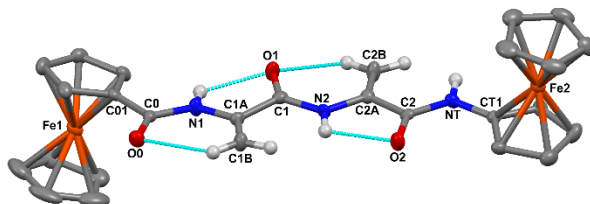
S. S. is grateful to the University of Padova for having supported this work through Grant P-DiSC-2018. B.B. and F.F. greatly acknowledge the joint support from Fresenius Kabi iPSUM and the University of Padova (Grant Uni-Impresa 2019, PEPTIND).

Keywords: didehydroalanine • dipole moment • ferrocene • flat peptides • foldamers

- [1] a) S. H. Gellman, *Acc. Chem. Res.* **1998**, *31*, 173-180; b) C. Z. Girvin, S. H. Gellman, *J. Am. Chem. Soc.* **2020**, *142*, 17211-17223.
- [2] B. A. F. Le Bailly, J. Clayden, *Chem. Commun.* **2016**, *52*, 4852-4863.
- [3] a) S. Hecht, I. Huc in *Foldamers: Structure, Properties, and Applications*; Wiley-VCH, Weinheim, **2007**, pp. 1-435; b) D. J. Hill, M. J. Mio, R. B. Prince, T. S. Hughes, J. S. Moore, *Chem. Rev.* **2001**, *101*, 3893-4011; c) C. G. Cummings, A. D. Hamilton, *Curr. Opin. Chem. Biol.* **2010**, *14*, 341-346; d) G. Guichard, I. Huc, *Chem. Commun.* **2011**, *47*, 5933-5941; e) T. A. Martinek, F. Fulop, *Chem. Soc. Rev.* **2012**, *41*, 687-702; (f) Y. Ferrand, I. Huc, *Acc. Chem. Res.* **2018**, *51*, 970-977; g) S. Algar, M. Martín-Martínez, R. González-Muñiz, *Eur. J. Med. Chem.* **2021**, *211*, 113015.
- [4] a) R. P. Cheng, S. H. Gellman, W. F. DeGrado, *Chem. Rev.* **2001**, *101*, 3219-3232; b) D. Seebach, A. K. Beck, D. J. Bierbaum, *Chem. Biodivers.* **2004**, *1*, 1111-1239; c) E. Torres, E. Gorrea, K. K. Burusco, E. Da Silva, P. Nolis, F. Rua, S. Boussert, I. Diez-Perez, S. Dannenberg, S. Izquierdo, E. Giralt, C. Jaime, V. Branchadell, R. M. Ortuno, *Org. Biomol. Chem.* **2010**, *8*, 564-575; d) K. Wright, M. Wakselman, J. P. Mazaleyrat, L. Franco, A. Toffoletti, F. Formaggio, C. Toniolo, *Chem. Eur. J.* **2010**, *16*, 11160-11166; e) P. G. Vasudev, S. Chatterjee, N. Shamala, P. Balaram, *Chem. Rev.* **2011**, *111*, 657-687; f) C. M. Grison, S. Robin, D. J. Aitken,

- Chem. Commun.* **2016**, *52*, 7802-7805; g) R. Misra, S. Dey, R. M. Reja, H. N. Gopi, *Angew. Chem. Int. Ed.* **2018**, *57*, 1057-1061; h) J. Gong, T. Eom, W. Lee, A. Roy, S. Kwon, H. Kim, H.-S. Lee, *ChemPlusChem* **2019**, *84*, 481-487; i) R. Bucci, A. Contini, F. Clerici, E. M. Beccalli, F. Formaggio, I. Maffucci, S. Pellegrino, M. L. Gelmi, *Front. Chem.* **2019**, *7*, Art. N. 192.
- [5] a) R. Kaul, P. Balaram, *Bioorg. Med. Chem.* **1999**, *7*, 105-117; b) C. Toniolo, M. Crisma, F. Formaggio, C. Peggion, *Biopolymers* **2001**, *60*, 396-419; c) A. Scarso, U. Scheffer, M. Gobel, Q. B. Broxterman, B. Kpatein, F. Formaggio, C. Toniolo, P. Scrimin, *Proc. Natl. Acad. Sci. USA* **2002**, *99*, 5144-5149; d) S. Yasutomi, T. Morita, Y. Imanishi, S. Kimura, *Science* **2004**, *304*, 1944-1947; e) C. Toniolo, M. Crisma, F. Formaggio, C. Peggion, Q. B. Broxterman, B. Kpatein, *J. Incl. Phenom. Macro.* **2005**, *51*, 121-136; f) C. Toniolo, F. Formaggio, B. Kpatein, Q. B. Broxterman, *Synlett.* **2006**, *9*, 1295-1310; g) M. Crisma, F. Formaggio, A. Moretto, C. Toniolo, *Biopolymers* **2006**, *84*, 3-12; h) F. Clerici, E. Erba, M. L. Gelmi, S. Pellegrino, *Tetrahedron Lett.* **2016**, *57*, 5540-5550; i) T. Narancic, S. A. Almahboub, K. E. O'Connor, *World J. Microb. Biot.* **2019**, *36*, 1917-1927; j) H. Yokoo, M. Hirano, T. Misawa, Y. Demizu, *ChemMedChem* **2021**, *16*, 1-9; k) U. Bachor, M. Maczynski, *Molecules* **2021**, *26*, 438.
- [6] a) D. Siodlak, *Amino Acids* **2015**, *47*, 1-17; b) S. Wang, Q. Fang, Z. Lu, Y. L. Gao, L. Trembleau, R. Ebel, J. H. Andersen, C. Phillips, S. Law, H. Deng, *Angew. Chem. Int. Ed.* **2021**, *60*, 3229-3237.
- [7] M. Crisma, F. Formaggio, C. Toniolo, T. Yoshikawa, T. Wakamiya, *J. Am. Chem. Soc.* **1999**, *121*, 3272-3278.
- [8] M. Crisma, F. Formaggio, C. Alemán, J. Torras, C. Ramakrishnan, N. Kalmankar, P. Balaram, C. Toniolo, *Pept. Sci.* **2018**, *110*, e23100.
- [9] a) C. Peggion, A. Moretto, F. Formaggio, M. Crisma, C. Toniolo, *Biopolymers* **2013**, *100*, 621-636; b) M. Tanaka, S. Nishimura, M. Oba, Y. Demizu, M. Kurihara, H. Suemune, *Chem. Eur. J.* **2003**, *9*, 3082-3090; c) K. A. H. Wildman, A. Ramamoorthy, T. Wakamiya, T. Yoshikawa, M. Crisma, C. Toniolo, F. Formaggio, *J. Pept. Sci.* **2004**, *10*, 336-341; d) M. Tanaka, *Chem. Pharm. Bull.* **2007**, *55*, 349-358; e) M. Crisma, A. Moretto, C. Peggion, L. Panella, B. Kpatein, Q. B. Broxterman, F. Formaggio, C. Toniolo, *Amino Acids* **2011**, *41*, 629-641; f) F. Formaggio, M. Crisma, C. Peggion, A. Moretto, M. Venanzi, C. Toniolo, *Eur. J. Org. Chem.* **2012**, 167-174; g) C. Peggion, M. Crisma, C. Toniolo, F. Formaggio, *Tetrahedron* **2012**, *68*, 4429-4433; h) F. Formaggio, M. Crisma, G. Ballano, C. Peggion, M. Venanzi, C. Toniolo, *Org. Biomol. Chem.* **2012**, *10*, 2413-2421; i) H. Maekawa, G. Ballano, C. Toniolo, N.-H. Ge, *J. Phys. Chem. B* **2011**, *115*, 5168-5182; j) H. Maekawa, G. Ballano, F. Formaggio, C. Toniolo, N.-H. Ge, *J. Phys. Chem. C* **2014**, *118*, 29448-29457.
- [10] a) J. R. Winkler, H. B. Gray, *J. Biol. Inorg. Chem.* **1997**, *2*, 399-404; b) H. B. Gray, *Science* **2005**, *307*, 99-102.
- [11] a) R. Improtà, S. Antonello, F. Formaggio, F. Maran, N. Rega, V. Barone, *J. Phys. Chem. B* **2005**, *109*, 1023-1033; b) F. Remacle, M. A. Ratner, R. D. Levine, *Chem. Phys. Lett.* **1998**, *285*, 25-33; c) G. Jones, L. N. Lu, H. Fu, C. W. Farahat, C. Oh, S. R. Greenfield, D. J. Gosztola, M. R. Wasielewski, *J. Phys. Chem. B* **1999**, *103*, 572-581; d) S. Antonello, F. Formaggio, A. Moretto, C. Toniolo, F. Maran, *J. Am. Chem. Soc.* **2003**, *125*, 2874-2875; e) F. Polo, S. Antonello, F. Formaggio, C. Toniolo, F. Maran, *J. Am. Chem. Soc.* **2005**, *127*, 492-493; f) S. Mehlhose, N. Frenkel, H. Uji, S. Hölzel, G. Müntze, D. Stock, S. Neugebauer, A. Dadgar, W. Abuillan, M. Eickhoff, S. Kimura, M. Tanaka, *Adv. Funct. Mater.* **2018**, *28*, 1704034; g) C. Zuliani, F. Formaggio, L. Scipionato, C. Toniolo, S. Antonello, F. Maran, *ChemElectroChem* **2020**, *7*, 1225-1237.
- [12] a) J. Jiao, G. J. Long, F. Grandjean, A. M. Beatty, T. P. Fehlner, *J. Am. Chem. Soc.* **2003**, *125*, 7522-7523; b) S. A. Serron, W. S. Aldridge, III, C. N. Fleming, R. M. Danell, M.-H. Baik, M. Sykora, D. M. Dattelbaum, T. J. Meyer, *J. Am. Chem. Soc.* **2004**, *126*, 14506-14514; c) J. X. Yu, J. R. Horsley, A. D. Abell, *Austral. J. Chem.* **2013**, *66*, 848-851; d) A. Shah, B. Adhikari, S. Martić, A. Munir, S. Shahzad, K. Ahmad, H. B. Kraatz, *Chem. Soc. Rev.* **2015**, *44*, 1015-1027; e) N. Amdursky, *ChemPlusChem* **2015**, *80*, 1075-1095; f) J. X. Yu, J. R. Horsley, A. D. Abell, *Acc. Chem. Res.* **2018**, *51*, 2237-2246.
- [13] a) G. Jaouen, *Bioorganometallics*, Wiley-VCH, New York, **2006**; b) H.-B. Kraatz, N. Metzler-Nolte, *Concepts and Models in Bioinorganic Chemistry*, Wiley-VCH, New York, **2006**; c) D. N. Van Staveren, N. Metzler-Nolte, *Chem. Rev.* **2004**, *104*, 5931-5985; d) S. Martić, M. Labib, P. O. Shipman, H.-B. Kraatz, *Dalton Trans.* **2011**, *40*, 7264-7290; e) R. Afrasiabi, H. B., Kraatz, *Chem. Eur. J.* **2013**, *19*, 17296-17300; f) N. Falcone, S. Basak, B. Dong, J. Syed, A. Ferranco, A. Lough, Z. She, H. B. Kraatz, *ChemPlusChem* **2017**, *82*, 1282-1289; g) S. Peter, B. A. Aderibigbe, *Molecules* **2019**, *24*, 3604-3631; h) Y. Feng, Y. Wang, J. Zhang, M. Wang, W. Qi, R. Su, Z. He, *Adv. Mater. Interfaces* **2019**, *6*, 1901082; i) N. C. S. Costa, J. P. Piccoli, N. A. Santos-Filhol, L. C. Clementino, A. M. Fusco-Almeida, S. R. De Annunzio, C. R. Fontana, J. B. M. Verga, S. F. Etol, J. M. Pizauro-Junior, M. A. S. Graminha, E. M. Cilli, *PLoS ONE* **2020**, *15*(3): e0228740; j) G. Zhang, J. Wang, Y. Wang, W. Qi, R. Su, Z. He, *ChemPlusChem* **2020**, *85*, 2341-2348.
- [14] a) N. Metzler-Nolte, M. Salmain, in *Ferrocenes: Ligands, Materials and Biomolecules* (Ed.: P. Štěpnička), Wiley, Chichester, UK, **2008**, pp. 499-639; b) S. Santi, A. Bisello, R. Cardena, A. Donoli, *Dalton T.* **2015**, *44*, 5234-5257; c) A. Donoli, A. Bisello, R. Cardena, M. Crisma, L. Orian, S. Santi, *Organometallics* **2015**, *34*, 4451-4463.
- [15] a) A. Donoli, V. Marcuzzo, A. Moretto, C. Toniolo, R. Cardena, A. Bisello, S. Santi, *Org. Lett.* **2011**, *13*, 1282-1285; b) A. Donoli, V. Marcuzzo, A. Moretto, M. Crisma, C. Toniolo, R. Cardena, A. Bisello, S. Santi, *Pept. Sci.* **2012**, *100*, 14-24.
- [16] a) N. Metzler-Nolte, S. I. Kirin, H.-B. Kraatz, *Chem. Soc. Rev.* **2006**, *35*, 348-354; b) L. Barišić, M. Čakić, K. A. Mahmoud, Y. Liu, H.-B. Kraatz, H. S. Pritzkow, I. Kirin, N. Metzler-Nolte, V. Rapić, *Chem. Eur. J.* **2006**, *12*, 4965-4980; c) T. Hirao, *J. Organomet. Chem.* **2009**, *694*, 806-811; d) D. Siebler, M. Linseis, T. Gasi, L. M. Carrella, R. F. Winter, C. Förster, K. Heinze, *Chem. Eur. J.* **2011**, *17*, 4540-4551; e) G. Angelici, M. Górecki, G. Pescitelli, N. Zanna, M. Monari, C. Tomasini, *Biopolymers* **2017**, e23072; f) T. Moriuchi, T. Nishiyama, Y. Tayano, T. Hirao, *J. Inorg. Biochem.* **2017**, *177*, 259-265.
- [17] a) Y. Arikuma, H. Nakayama, T. Morita, S. Kimura, *Langmuir* **2011**, *27*, 1530-1535; b) Y. Arikuma, H. Nakayama, T. Morita, S. Kimura, *Angew. Chem. Int. Ed.* **2010**, *49*, 1800-1804.
- [18] D. F. Kennedy, M. Crisma, C. Toniolo, D. Chapman, *Biochemistry* **1991**, *30*, 6541-6548.
- [19] a) A. Houlton, C. J. Isaac, A. E. Gibson, B. R. Horrocks, W. Clegg, M. R. J. Elsegood, *J. Chem. Soc., Dalton Trans.* **1999**, 3229-3234; b) H.-B. Kraatz, *J. Inorg. Organomet. Polym. Mater.* **2005**, *15*, 83-106.
- [20] a) R. A. Engh, R. Huber, *Acta Crystallogr. A* **1991**, *47*, 392-400; b) D. E. Tronud, P. A. Karplus, *Acta Crystallogr. D* **2011**, *67*, 699-706.
- [21] R. W. Newberry, R. T. Raines, *Nat. Chem. Biol.* **2016**, *12*, 1084-1088.
- [22] M. C. Burla, R. Caliandro, B. Carrozzini, G. L. Casciarano, C. Cuocci, C. Giacovazzo, M. Mallamo, A. Mazzone, G. Polidori, *J. Appl. Crystallogr.* **2015**, *48*, 306-309.
- [23] G. M. Sheldrick, *Acta Crystallogr. C* **2015**, *71*, 3-8.
- [24] C. Amatore, C. Lefrou, F. Pflüger, *J. Electroanal. Chem.* **1989**, *270*, 43-59.

Entry for the Table of Contents



Flat foldamers, adopting the peptide 2.0_5 -helix, were covalently bound to two ferrocene moieties, as redox probes. These conjugates preserve the flat and extended conformation both in solution and in the crystal state (X-ray diffraction of single crystals). Cyclic voltammetry measurements are in agreement with the adoption of the 2.0_5 -helix, characterized by a negligible dipole moment. Thus, this type of elongated, α -peptide foldamer is acting as an insulators rather than a charge conductor.